Inclusion Complexes of 6-Bromo-2-Naphthol (Guest) and α-Cyclodextrin (Host): Thermodynamics of the Binary Complex and First-Reported Dynamics of a Triplet-State Guest/Host$_2$ Complex†

R. Elizabeth Brewster, Benjamin F. Teresa, and Merlyn D. Schuh*

Department of Chemistry, POB 7120, Davidson College, Davidson, North Carolina 28035-7120

Received: February 26, 2003; In Final Form: June 17, 2003

The thermodynamics properties of the 1 guest−1 host ground-state complex were determined from near UV absorbance measurements as a function of temperature. Entropy changes for formation of the binary and ternary complexes suggest that the brominated end of the guest molecule is attached to the first host molecule, and the hydroxyl end is encapsulated by the second host. The enthalpy of stabilization is approximately twice as great for the ternary complex as for the binary complex in the ground state. A molecular kinetics mechanism is presented that is used to determine some of the dynamics properties of the 1 guest−2 host complex from measurements of the pulsed laser-induced phosphorescence that emanates from the triplet state of 6-bromo-2-naphthol. The rate of dissociation of the triplet-state ternary complex is governed by a large Arrhenius activation energy (82 ± 1 kJ/mol), and the dissociation rate constant (k_{-d} = 8400 s^{-1} at 25 °C) is more than an order of magnitude smaller than that in typical binary complexes of cyclodextrins. It is suggested that the apparent increased stability of the ternary complex over the binary complex is due to general van der Waals interactions and/or hydrogen bonding between host molecules.

Introduction

The most abundant natural cyclodextrins are cyclic oligosaccharides composed of 6, 7, or 8 α-(1,4)-linked glucopuranose rings that are referrred to as α-, *β*-, and *γ*-cyclodextrins. The structures are "fairly" rigid and have a unique molecular architecture that resembles a hollow truncated cone or torus with end diameters of 5−8 Å determined by the number of glucose units.

Secondary hydroxyl groups and primary hydroxyl groups, which line the larger and smaller circumferences, respectively, produce a relatively hydrophilic exterior and make cyclodextrins water soluble. However, C3−H, C5−H, and C6−H_2 hydrogens and the ether-like O4 oxygens make the cyclodextrin cavity relatively hydrophobic in character. As a result, cyclodextrins serve well as host molecules in forming inclusion complexes with a large number of guest molecules of the appropriate size and polarity. Such cyclodextrin complexes have been used in food, cosmetic, and toiletry applications,[1−3] in drug stabilization and delivery technology,[4,5] in pesticide formulations, by biotechnological industries,[1,2] for analytical applications,[6] as models in the field of molecular recognition, and to model enzyme behavior, including both substrate complexation and reactivity.[7] Although most such complexes have consisted of a single guest molecule inside a single host, particular polyrotaxanes consisting of two or more cyclodextrin molecules that slide along a single long-chain guest molecule have been used in supramolecular chemistry as possible simple molecular machines.[8]

The ability to rationally design cyclodextrin-guest inclusion complexes will ultimately require an understanding of the dynamics and thermodynamics factors controlling the formation and stabilization of complexes. Considerable thermodynamics information has been obtained for 1:1 guest−host complexes and for very few ternary complexes.[9−12] However, little kinetics information has been obtained about the dynamics (rate constants of formation and dissociation) of any complexes. The few reported rate constants for formation and dissociation have been primarily for 1:1 complexes involving triplet-state guest molecules, and no dynamics information has been reported for 1:2 (guest:host) complexes.[13−17] Such complexes may have considerable importance in the development of polyrotaxanes and may provide new practical applications, due to the additional protection of the guest molecule that is not provided by a single cyclodextrin molecule in a 1:1 complex.

Hamai has reported that aerated solutions of 6-bromo-2-naphthol (N) and α-cyclodextrin (C) produce phosphorescence, which has been shown from a range of spectroscopic experiments to emanate exclusively from single N molecules that are well protected between two Cs in a 1 guest−2 host complex.[18,19] Moreover, the 1:1 complex formed between 1-bromonaphthalene and *β*-cyclodextrin is phosphorescent only in nitrogen-purged solutions.[17] Also, the long-lived phosphorescence, from what is believed to be the 1:1 complex of N and *β*-cyclodextrin, has been observed only in nitrogen-purged solutions.[20] NMR spectra for the naphthalene hydrogens show that the brominated end of ground-state N binds first to the host, and the hydroxyl end binds second.[19] A reasonable interpretation of this result is that the hydrophobic Br end of N interacts with the first C by entering its hydrophobic cavity, and the hydroxyl end of N gains stability and maximum protection from the solvent by entering, at least part way, the core of the second C molecule. These experiments do not allow a determination of the depth to which each end of the N molecule penetrates the core of each C. Moreover, the dimensions of the cavity of one C are sufficiently large to accommodate most of the entire N molecule when its long axis is approximately parallel to the axis extending through the center of the two openings of C. So the hydroxyl end of N can conceivably form a surface interaction through hydrogen

† Part of the special issue "Charles S. Parmenter Festschrift".

* Corresponding author. meschuh@davidson.edu

10.1021/jp030253p CCC: $25.00
Published on Web 08/29/2003

bonds between the hydroxyl of N and the hydroxyl(s) of the second C molecule. Such geometry could still provide protection of N from the solvent without deep penetration into the core of the second C.

To begin learning about the thermodynamics and dynamics of ternary complexes, we have begun studies of complexes formed between phosphorescent bromonaphthalene derivatives and α-cyclodextrin. It was reported that the phosphorescence lifetime of the $^3NC_2$ complex, where ^3N represents the triplet state guest molecule, decreases by more than 2 orders of magnitude over the temperature range 1.6−59.7 °C.[21] The present paper reports on the molecular dynamics of the $^3NC_2$ complex and is the first such report about a 1 guest−2 host ternary complex. The binding constants for formation of the ground-state 1:1 and 1:2 complexes as a function of temperature are also reported. An additional purpose of this paper is to describe the experimental method and establish the chemical kinetics analysis being used to determine the dynamics of other ternary complexes.

Although triplet−triplet absorption experiments allow the direct measurement of the kinetic behavior of a triplet state molecule, the use of such experiments in the present study would be limited by the ability to resolve the overlapping triplet−triplet absorption spectra and time evolution of both the binary and ternary triplet state complexes. The experimental method described herein has the advantage of detecting the phosphorescence of a single species, namely the ternary complex.

Experimental Section

Model for Complex Formation. Because bimolecular events are kinetically much more likely than termolecular events, the formation of complexes between N and C is proposed to occur by the following mechanism. The 3 superscript refers to the triplet state of N; k_a, k_{-a}, k_d, and k_{-d} designate the rate constants for formation and dissociation of the binary and ternary complexes involving triplet-state N, respectively; K_1 and K_2 are the binding constants for the formation of the ground-state binary complex NC and ternary complex NC_2, respectively; and k_o, k', and k'' are the unimolecular (or pseudo-unimolecular) decay rates of triplet-state N in uncomplexed form, within the binary complex, and within the ternary complex, respectively. k'' includes the phosphorescence decay rate of $^3NC_2$.

$$\begin{array}{ccccc} & k_a & & k_d, +C & \\ C + {}^3N & \rightleftharpoons & {}^3NC & \rightleftharpoons & {}^3NC_2 \\ & k_{-a} & & k_{-d} & \\ k_o \downarrow \uparrow h\nu & & k' \downarrow \uparrow h\nu & & k'' \downarrow \uparrow h\nu \\ & K_1 & & K_2, +C & \\ C + N & \rightleftharpoons & NC & \rightleftharpoons & NC_2 \end{array}$$

Because the pK_a of the hydroxyl group of N has been measured to be 9.2,[18] the dominance of only the protonated form of N is assured in neutral aqueous solutions. Furthermore, the characteristic fluorescence peaks for the naphthol (350 nm) and naphtholate ions (420 nm) have been used to show that ionization of free N is absent in neutral nonbuffered aqueous solution and remains suppressed in complexes with C.[19,22]

Because $[C]_o \gg [N]_o$ for the experiments described herein, the total light absorbance by both uncomplexed N and N within the complexes can be expressed by eq 1.

$$A = \frac{[N]_o(\epsilon_o + \epsilon_1 K_1[C]_o + \epsilon_2 K_1 K_2 [C]_o^2)}{(1 + K_1[C]_o + K_1 K_2 [C]_o^2)} \qquad (1)$$

where ϵ_o, ϵ_1, and ϵ_2 are the molar absorptivities for N, NC, and NC_2, respectively.[18] As in refs 18 and 19, the absorbance was measured at 345 nm, the wavelength at which the maximum change in absorbance occurs upon complexation of N with C.

For absorbance data at each temperature, a method similar to that described in ref 18 was used to evaluate K_1 and K_2 from eq 1. Unique values of ϵ_o and ϵ_2 were determined by extrapolation of [C] to zero and infinity, respectively. The values of ϵ_1, K_1 and K_2 were then varied to achieve the best fit. Such a fitting procedure can be criticized, because the values of ϵ_1, K_1, and K_2 so obtained are not unique. However, this nonuniqueness is not strictly true for the K_1 and K_2 values reported herein because it was found that they also gave essentially the best fit to eq 2, which is a mathematically independent equation for the intensity of phosphorescence, I_p, that is derivable for the proposed complex formation model.[18] The good fit of experimental phosphorescence intensity to eq 2, using K_1 and K_2 values (obtained by fitting to eq 1), was noted at three temperatures in the present study. Because all values of K_1 and K_2 obtained from eq 1decrease smoothly and monotonically with temperature, it is reasonable to assume that the values of these binding constants fit eq 2 at the other temperatures as well.

$$I_p = \frac{[N]_o K_1 K_2 [C]_o^2}{(1 + K_1[C]_o + K_1 K_2 [C]_o^2)} \qquad (2)$$

The kinetics analysis of the triplet-state complex is an extension of that first used in ref 23 to analyze the kinetically similar complex formation involving ionic micelles in aqueous solution and later used to analyze other triplet-state binary complexes of cyclodextrins, for example as in refs 15, 17, 24, and 25.

The laser excitation pulse populates the first excited singlet state of both uncomplexed and complexed N molecules. A large fraction of these molecules undergoes intersystem crossing to the triplet state. It is assumed that the starting population of triplet-state molecules is established during the nsec duration of the laser pulse at time zero. This assumption is supported by the absence of a transient increase in phosphorescence more than one μsec after the laser pulse.

The relative amounts of ^3N, ^3NC, and $^3NC_2$ are calculated as follows. The concentrations of ground-state N, NC, and NC_2 are determined by using the K_1 and K_2 values published in the literature or obtained in the present work (*vide infra*) to solve the chemical equilibria equations. The fractions of N, NC, and NC_2 molecules that are raised to the first excited singlet state by light absorption at the excitation laser wavelength are determined by using the molar absorptivities either reported in ref 18 or determined herein (vide infra). In view of the protection from quenching of ^3N provided by complexation with C, it is reasonable to assume that the rate of intersystem crossing from the first excited singlet state of N should be at least equal if not greater for N in the NC and NC_2 complexes than for unbound N. With this assumption, it is calculated that for nearly all of the C concentrations used in the experiments the laser pulse produces a population of excited triplet-state species for which more than ninetyfive percent of the ^3N molecules are bound in either the binary or ternary complex. The single exception occurs with the C concentration of 0.9 mM for which over sixtyfive percent of the ^3N molecules are complexed. Yet, the good curve fit of the data for each plot in Figure 4 shows that the kinetics behavior at a C concentrations of 0.9 mM and higher is the same, within experimental limits of detection (vide infra). Thus, only the equilibrium between the binary and ternary complexes

needs to be considered in the kinetics model, for which the rate equations are

$$\frac{d[^3NC]}{dt} = k_{-d}[^3NC_2] - (k_{-a} + k' + k_d[C])[^3NC] \quad (3)$$

$$\frac{d[^3NC_2]}{dt} = k_d[^3NC][C] - (k_{-d} + k'')[^3NC_2] \quad (4)$$

^3NC molecules have less protection from quenching than do $^3NC_2$ molecules, as is indicated by the fact that phosphorescence is observed from only the ternary $^3NC_2$ complex in aerated solutions. Thus, the pseudo-unimolecular decay rate of ^3NC is dominated by oxygen quenching in aerated solutions, and it is reasonable to assume that $k'' \ll k'$. This condition guarantees that $[^3NC]$ is much less than $[^3NC_2]$ and justifies application of the steady-state approximation to $[^3NC]$. Solution of rate eqs 3 and 4 produces the integrated rate equation for $[^3NC_2]$, which is found to decay single-exponentially with a phosphorescence lifetime, τ_p, given by eq 5.

$$1/\tau_p = k'' + k_{-d} - \frac{k_{-d}[C]}{(k_{-a} + k')/k_d + [C]} \quad (5)$$

Because $[C]_o \gg [N]_o$, the values of [C] in eq 5 are essentially the same as $[C]_o$. The form of eq 5 shows that $1/\tau_p$ should decrease from a value of $k'' + k_{-d}$ when $[C] = 0$ to a limiting value of k'' as [C] approaches infinity, and k_{-d} is the difference between extrapolated values. Equation 5 is rearranged to eq 6, which shows a linear relationship between the left-hand side and [C].

$$\frac{1}{(1/\tau_p - k'')} = \frac{k_d[C]}{(k_{-a} + k')k_{-d}} + \frac{1}{k_{-d}} \quad (6)$$

The left-hand side of eq 6 is plotted versus [C] for different values of *k*". The best value of k'' is that for which the plot is linear and also has an intercept, $1/k_{-d}$, for which k_{-d} is in reasonable agreement with the difference between $1/\tau_p$ values when [C] is extrapolated to zero and infinity. Equation 7 follows from eq 6 and shows that k_d can be obtained if $k_{-a} + k'$ is known.

$$k_d = (\text{slope/intercept})(k_{-a} + k') \quad (7)$$

The value of $k_{-a} + k'$ could not be determined from the experiments described herein. Although the value could be estimated from the corresponding experimental value for similar molecular complexes, $k_{-a} + k'$ has not been reported for any molecular complexes deemed to be sufficiently similar to the ^3NC complex to provide a reliable estimate. Thus, the present work reports explicit values for only k_{-d} and k''.

Chemicals and Sample Preparation. 6-Bromo-2-naphthol was obtained from Aldrich, and α-cyclodextrin was a generous gift from Cerestar USA, Inc. of Indianapolis (lot no. G 8071−2). Both chemicals were used without further purification. Water was deionized with a Barnstead EASY pure water purification system and typically had a resistivity of 18 MΩ cm. Samples were thermostated to within 0.1 °C in a metal housing, through which water flowed from a temperature-regulated circulating water bath. Solutions were prepared as follows: A solution of weighed N was prepared that had a peak absorbance the same as that reported in ref 18 to have a concentration of 9×10^{-5} M. A stock solution, containing 0.10 M α-cyclodextrin, was prepared by dissolving a weighed amount of α-cyclodextrin in the N-containing solution. Samples for doing absorbance and phosphorescence measurements were prepared by serial dilution of the stock solution with different volumes of the N-containing solution. For both absorbance and phosphorescence measurements, each sample was contained in a 1-cm^2 quartz cuvette, stoppered by a Teflon plug fitted into a ground-glass opening.

Hazard. 6-Bromo-2-naphthol is possibly carcinogenic in humans. It may cause eye irritation and skin irritation. It is advisable that it be used in a hood and handled with gloved hands.

Instrumentation and Data Analyses. A Perkin-Elmer Lambda 6 UV/visible spectrophotometer was used to record absorption spectra. Changes in absorbance as a function of α-cyclodextrin concentration were measured at a wavelength of 345 nm.

The excitation instrumentation used to do transient phosphorescence measurements has been described previously.[26] The frequency-doubled output from a Spectra Physics model GCR150 Nd:YAG laser was used to pump a Spectra Physics PDL3 dye laser. The output of the dye laser was frequency doubled and tuned to 345 nm. The resulting excitation pulses had a duration of 6 ns (fwhm), a bandwidth of 0.4 cm^{-1}, a pulse rate of 10 Hz, a focused beam diameter of about 7 mm, and were adjusted to an energy of a few mJ per pulse. Phosphorescence pulses were focused through a fast camera lens into a 0.25 m Jarrell Ash spectrometer, amplified by a fast-response EMI 9798 QB photomultiplier and recorded on a Tektronix model TDS 620 oscilloscope. For each phosphorescence lifetime measurement, 200−800 oscilloscope traces were signal-averaged, and the initial intensity of phosphorescence decay was followed over 2−3 orders of magnitude. Each phosphorescence decay profile was digitized and consisted of 300−400 points. From the same oscilloscope traces, the relative phosphorescence intensities, I_p, were also measured as the areas under the traces.

It was found experimentally that A_{345} for samples containing C and N changes by less than five percent over the temperature range 1.6−50 °C, suggesting that the values of ϵ_o, ϵ_1, and ϵ_2 change individually by only a few percent. Thus, self-consistent fits of A_{345} data to eq 1 for all experimental temperatures were found to be possible by using a range of values for ϵ_o, ϵ_1, and ϵ_2 that were within 3.6%, 6.9%, and 4.9% of the mean values of these molar absorptivities ($\epsilon_o = 420$ M^{-1} cm^{-1}, $\epsilon_1 = 750$ M^{-1} cm^{-1}, and $\epsilon_2 = 1750$ M^{-1} cm^{-1}), respectively.

Signal-averaged phosphorescence traces were stored on a microcomputer hard drive, and the phosphorescence signals were fitted by a multiexponential or single-exponential fitting routine of Sigma Plot software. With the exception of phosphorescence signals recorded at 1.6 °C, the phosphorescence signals were fitted well by a single exponential. The signals for most α-cyclodextrin concentrations at 1.6 °C were fitted best by a double-exponential. However, the two lifetime components did not show a monotonic change with increasing α-cyclodextrin concentration and did not yield self-consistent results. So, such data were fitted by single exponentials, and the reciprocal lifetimes showed the expected monotonic decrease with increasing α-cyclodextrin concentration. Furthermore, all of the single-exponential lifetimes for samples at 1.6 °C had correlation coefficients greater than 0.997, and the plot of $1/\tau_p$ versus [C] was consistent with the corresponding plots at the other temperatures.

Because the value of each rate constant was obtained by fitting lifetime data to eq 6 rather than by direct experimental measurement, it was expedient to determine the propagation of

TABLE 1: Thermodynamics Properties for Ground-State Binary and Ternary Complexes

K_1(25 °C)[a]	$\Delta G_1°$ (kJ/mol)	$\Delta H_1°$ (kJ/mol)	$\Delta S_1°$ (J/mol-K)	K_2 (25 °C)[a]	$\Delta G_2°$ (kJ/mol)	$\Delta H_2°$ (kJ/mol)	$\Delta S_2°$ (J/mol-K)
460 ± 20	−15.2 ± 0.1	−25.9 ± 1.1	−36 ± 4	650 ± 50	−16.0 ± 0.2	−54.4 ± 2.5	−129 ± 9

[a] Values of K have units of M^{-1} and were obtained from van't Hoff plots.

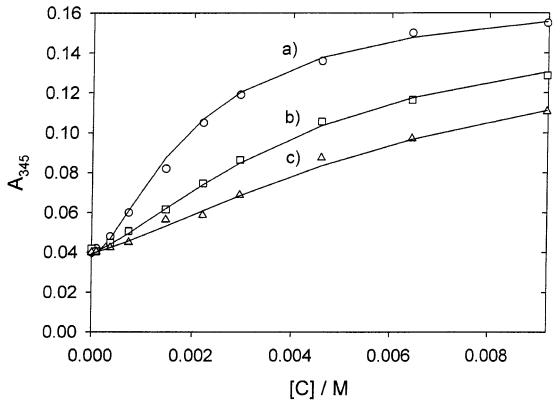

Figure 1. Absorbance at 345 nm as a function of α-cyclodextrin concentration and temperature. The 6-bromo-2-naphthol concentration was 9×10^{-5} M. (a) 23.0 °C, (b) 35.4 °C, (c) 44.0 °C. The curves through the data points were obtained by using the optimal values of ϵ_o, ϵ_1, ϵ_2, K_1, and K_2 for each temperature in eq 1.

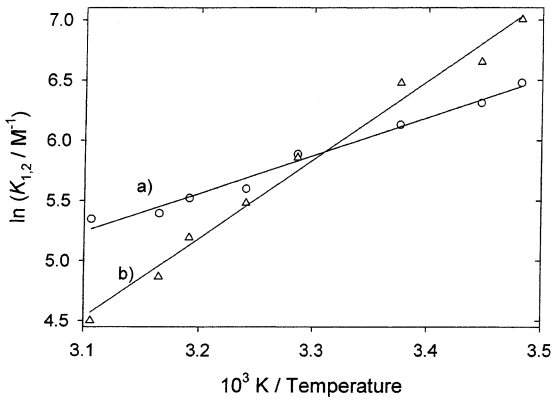

Figure 2. van't Hoff plots for the ground-state binding constants of the (a) binary complex, K_1, and (b) ternary complex, K_2.

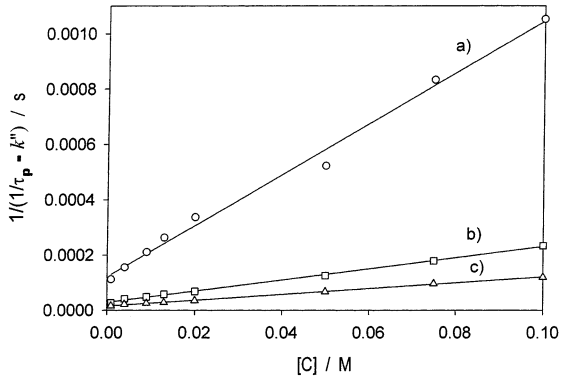

Figure 3. The left-hand side of eq 6 plotted versus α-cyclodextrin concentration for that value of k'' that made the plot optimally linear for samples at (a) 25.0 °C, (b) 39.4 °C, and (c) 45.8 °C. The 6-bromo-2-naphthol concentration was 9×10^{-5} M. The curves through the data points are the linear regression plots.

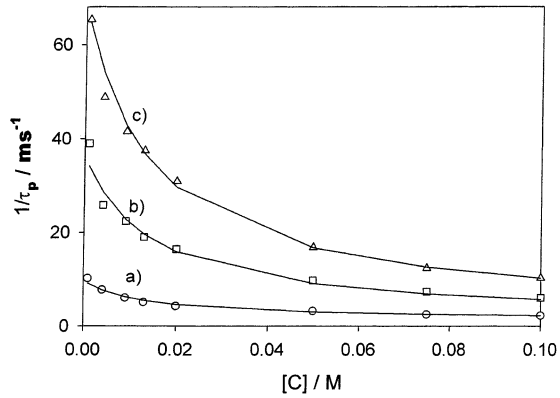

Figure 4. Reciprocal phosphorescence lifetime versus the α-cyclodextrin concentration for samples thermostated at (a) 25.0 °C, (b) 39.4 °C, and (c) 45.8 °C. The 6-bromo-2-naphthol concentration was 9×10^{-5} M. The curves through the data points were obtained by substituting into eq 5 the values of k'', k_{-d}, and $(k_{-q} + k')/k_d$, obtained from the optimally linear fitting of lifetime data to eq 6.

error by using a graphical method. Although a single value of k'' gave the highest correlation coefficient for the fitting of each set of lifetime data to eq 6, usually a range of k'' values was produced that had nearly as good fits with acceptable correlation coefficients. For data at each temperature, that value of k'' was selected for which the slope and intercept of the plot gave a value k_{-d} that was consistent with the monotonic trend displayed by this rate constant over the temperature range. For each temperature, in addition to the chosen fitted plot, two more fitted plots were constructed that had the largest and smallest slopes, corresponding to two k'' values within the range of reasonable values. These two values gave the range of uncertainty for k''. From the intercepts of these two plots the range of uncertainty associated with k_{-d} was estimated. For each Arrhenius plot, corresponding to the triplet-state complex, the extrema associated with each data point corresponded to this range of uncertainty. The following method was used to estimate the uncertainty in values of K_1 and K_2 at each temperature. For each set of K_1 and K_2 values, the residuals were calculated for the difference between experimental absorbances and the values predicted from eq 1. Those sets of K_1 and K_2 values that had the similar lower residuals gave the ranges (uncertainties) of K_1 and K_2 values. The uncertainties in $\Delta H_1°$ and $\Delta H_2°$ were determined from the standard deviations of the slopes of van't Hoff plots.

Results

Figure 1 shows plots for different temperatures of the absorbance at 345 nm versus $[C]_o$ and corresponding curves fitted to eq 1. Figure 2 shows van't Hoff plots for values of K_1 and K_2 obtained from fitting data to eq 1. The enthalpies of formation obtained from the slopes of the plots in Figure 2, the values of K_1 and K_2 obtained at 25 °C, and other thermodynamics properties are presented in Table 1. $\Delta G°$ and $\Delta S°$ were obtained from $-RT \ln K$ and $\Delta G° = \Delta H° - T\,\Delta S°$, respectively.

Figure 3 shows the data for three temperatures fitted to eq 6 by using the fitting method described in the Experimental section. Figure 4 shows $1/\tau_p$ plotted versus [C] at three temperatures. The values of k_{-d} and k'' obtained from the plot for 25.0 °C in Figure 3 are given in Table 2. Arrhenius plots for k_{-d} and k'' are shown in Figure 5, and the Arrhenius activation energies are given in Table 2.

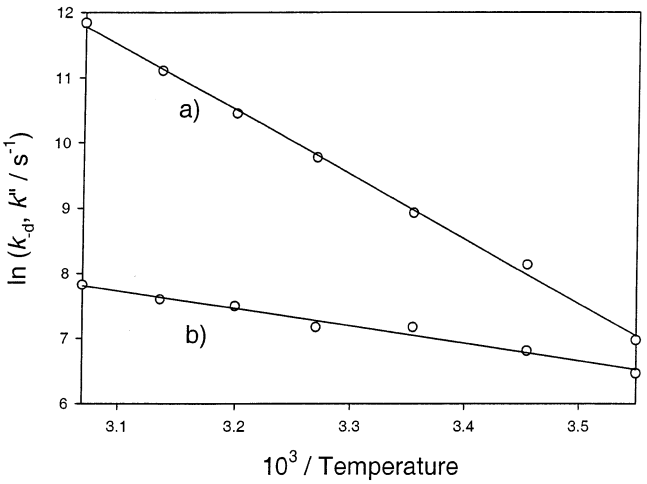

Figure 5. Arrhenius plots for the values of (a) k_{-d} and (b) k''.

TABLE 2: Kinetics Properties for Triplet-State Ternary Complex (25 °C)

k_{-d} ($\times 10^{-3}$ s^{-1})	$E_{a(-d)}$ (kJ/mol)	k'' ($\times 10^{-3}$ s^{-1})	$E_{a('')}$ (kJ/mol)
8.4 ± 1.5	82 ± 2	1.3 ± 0.15	23 ± 3

Discussion

The agreement is good between the values reported herein (*vide supra)* and in ref 18 for ϵ_o, ϵ_1, ϵ_2, K_1 and K_2 (500 M^{-1} cm^{-1}, 930 M^{-1} cm^{-1}, 2730 M^{-1} cm^{-1} and 560 M^{-1} and 530 M^{-1}, respectively). The relatively small differences between Hamai's values and the values reported herein (Table 1) are likely due to the uncertainty in the concentration of N, which arises due to its low aqueous solubility, and the variation in hydration level of the C. In Table 1, the size of $\Delta H_1°$ for binding of the first host molecule to N is typical for 1:1 cyclodextrin complexes and likely reflects stabilization primarily due to general van der Waals interactions similar to those present in other cyclodextrin complexes. For instance, $\Delta H°$ has been reported to be − 25.6 kJ/mol and −26.8 kJ/mol for the 1:1 complexes of 4-bromophenol−α-cyclodextrin and 2-naphthol/*β*-cyclodextrin, respectively.[27,28]

Perusal of Table 1 in ref 29, which lists thermodynamics properties for well over one thousand 1:1 complexes involving a range of guest molecules and either α-, *β*-, or *γ*-cyclodextrin, shows only seven other guest molecules that have stabilization enthalpies comparable to or greater than $\Delta H_2°$ for the ternary NC_2 complex (e.g., $\Delta H°$ equals −79.1 kJ/mol and −70.7 kJ/mol for α-cyclodextrin complexes with anthracene and nonanedioic acid, respectively[30,31]). Thus, in general, only guest molecules with greater length or size than N can be complexed with a single cyclodextrin host molecule and have an enthalpic stabilization comparable to that for NC_2, and it seems that interaction of N with the second C molecule is responsible for the value of $\Delta H_2°$ being approximately twice that of $\Delta H_1°$ in Table 1. If the larger value of $\Delta H_2°$ in Table 1 is due to general nondirected van der Waals interactions at similar distances between the guest molecule and both C molecules, then it can be concluded that the surface area of N that comes into contact with the second host molecule is approximately twice the contact area between N and the host C molecule in the binary complex. This interpretation is consistent with the minimum potential energy structures, predicted from a dynamic Monte Carlo method, for binary and ternary complexes of naphthalene with one and two α-cyclodextrins, respectively.[32] For the 1:1 complex, naphthalene is hindered from deep penetration into α-cyclodextrin and is merely attached to the secondary hydroxyls of the wider rim of the host. In the ternary complex, naphthalene is more deeply buried in the core of each host molecule and makes significant contact with the two host molecules. Alternatively, the large value of $\Delta H_2°$ could be attributable at least in part to hydrogen bonding between the two C molecules in the ternary complex This interpretation is consistent with the structure of the theoretical ternary complex between naphthalene and C molecules in which the rims of the large openings of the C molecules are sufficiently close for the formation of hydrogen bonds between the secondary hydroxyls of the host molecules.[32] However, the $\Delta H°$ values in Table 1 are not sufficiently specific to rule out the possible structure described in the Introduction in which the bromine end of N is deeply buried in the core of one C, but the hydroxyl end interacts only with the surface of the second C.

The entropy changes for binding the two host molecules can help to distinguish which ends of the N molecule are bound by the first and the second host molecules. $\Delta S_2°$ is substantially more negative than $\Delta S_1°$ and shows that the internal freedom of motion is much more restricted for binding of the second host than for binding of the first host. The interaction of the brominated end of N with C occurs via nondirected van der Waals interactions and should be subject to less restriction of motion than should the 2-hydroxyl group if it interacts with the C molecule through hydrogen bonds, which are generally regarded as being more directed. Thus, the relative values of $\Delta S_1°$ and $\Delta S_2°$ indicate that the brominated end of ground-state N binds the first host, and the hydroxyl end of N binds the second host molecule. This binding sequence is the same as that concluded on the basis of the NMR spectra for the naphthalene hydrogens.[19]

k'' equals the sum of all unimolecular decay processes for the triplet state of N, for which it can readily be shown, in general, that the overall activation energy, $E_{a('')}$, is given by the weighted sum $\sum_i k_i E_i / \sum_i k_i$, where k_i is rate constant for process i. In deaerated aqueous solution, the unimolecular photodissociative process is sufficiently active in unbound ^3N molecules that phosphorescence is undetectably weak.[19] The readily observed phosphorescence of $^3NC_2$ indicates that the photodissociation of ^3N is less active in the ternary complex due to a sharp increase in the activation energy of photodissociation. Therefore, the relatively small value for $E_{a('')}$ in Table 2 is dominated by the radiationless processes with small activation barriers. From Table 2, it is apparent that decay of the ternary complex is dominated by dissociation, k_{-d}, throughout most of the temperature range of our experiments. As in the case of the discussion of $\Delta H_2°$ above, the large value of $E_{a(-d)}$ is not yet understood but may in part be due to hydrogen bonds between the two host molecules of the ternary complex.

Far fewer thermodynamics and dynamics properties are available for ternary complexes that can be compared to the values of K_2 and $\Delta H_2°$ in Table 1 and the properties in Table 2. However, due to the structural similarities between N and 1-naphthyl-1-ethanol (1-NpOH) and 2-naphthyl-1-ethanol (2-NpOH), insights can be gained from a consideration of complexes between *β*-cyclodextrin and 1-NpOH and 2-NpOH. The average value of the binding constants for the 1:1 complex of the enantiomeric forms of 1-NpOH (160 M^{-1}) and 2-NpOH (800 M^{-1}) do not differ dramatically from K_1 (Table 1).[15] This result suggests that the strength of interactions within the three binary complexes are similar. However, the rates of dissociation (k_-) for the triplet-state complexes of 1-NpOH (4.8×10^5 s^{-1}) and 2-NpOH (1.8×10^5 s^{-1}) exceed by more than 20-fold the

value of k_{-d} for $^3NC_2$. This result shows the apparent enhanced stability of a ternary versus binary complex.

The dramatic reduction in the dissociation rate, k_{-d}, for the ternary complex $^3NC_2$ relative to other triplet-state binary complexes involving β-cyclodextrin is clear in refs 13, 14, and 33. N is less structurally similar to the guest molecules xanthone, flavone, chromone, and 4-vinylanisole in these binary complexes, and the possible effect on k_{-d} of added quencher (e.g., 0.5 M Na_2SO_4) in the solutions of some of the studies is not well understood. Nevertheless, the k_{-d} values (ranging from 4.4×10^6 s^{-1} for flavone to 21×10^6 s^{-1} for chromone) are several orders of magnitude larger than the value for $^3NC_2$ and emphasize the significance of the presence of the second cyclodextrin host molecule in reducing the rate of dissociation of the complex.

Finally, 2-NpOH also forms a 2:2 ground-state complex with β-cyclodextrin for which the binding constant is about 3000 M^{-1} and the rate of dissociation is estimated to be about 1000 s^{-1},[15] which is about eight times smaller than the k_{-d} value reported for the ternary complex $^3NC_2$. The cause for this dramatic decrease in the dissociation rate with increasing number of molecules in the complex in going from binary to ternary to quaternary complex is uncertain and may be due in part to whether the guest molecule is in the triplet state or ground state. Nevertheless, the decrease in k_{-d} clearly shows that the number of complex-stabilizing interactions increases as an additional host and then an additional guest is introduced into the complex. Moreover, the more molecules involved in the complex, the greater becomes the intermolecular surface contact for involvement of generalized van der Waals interactions and/or specific hydrogen-bonding interactions between the hydroxyl groups on each guest molecule and on the host molecules.

Acknowledgment. The authors thank the donors of the Petroleum Research Fund, administered by the American Chemical Society, for supporting this research. We also thank Cerestar, Inc. for the generous donation of the α-cyclodextrin used in this research.

References and Notes

(1) Szejtli, J., Osa, T. *Comprehensive Supramolecular Chemistry*; Pergamon: Oxford, 1996; Vol. 3 (Cyclodextrins), p 693.

(2) Szejtli, J. *Cyclodextrin Technology*; Kluwer Academic Publisher: Dordrecht, 1988; p 450.

(3) Szejtli, J. *J. Mater. Chem.* **1997**, *7*, 575−587.

(4) Uekama, K.; Hirayama, F.; Irie, T. *Chem. Rev.* **1998**, *98*, 2045−2076.

(5) Hedges, A. R. *Chem. Rev.* **1998**, *98*, 2035−2044.

(6) Li, S.; Purdy, W. C. *Chem. Rev.* **1992**, *92*, 1457−1470.

(7) Bender, M. L.; Komiyama, M. *Cyclodextrin Chemistry*; Springer-Verlag: Berlin, 1978.

(8) Harada, A. *Acc. Chem. Res.* **2001**, *34*, 456−464.

(9) Rekharsky, M. V.; Inoue, Y. *Chem. Rev.* **1998**, *98*, 1875−1917.

(10) Jobe, D. J.; Verrall, R. E.; Palepu, R.; Reinsborough, V. *J. Phys. Chem.* **1988**, *92*, 3582−3586.

(11) Bonomo, R. P.; Cucinotta, V.; D'Alessandro, F.; Impellizzeri, G.; Maccarrone, G.; Vecchio, G.; Rizzarelli, E. *Inorg. Chem.* **1991**, *30*, 2708−2713.

(12) Herrmann, W.; Wehrle, S.; Wenz, G. *J. Chem. Soc., Chem. Commun.* **1997**, 1709−1710.

(13) Liao, Y.; Frank, J.; Holzwarth, J. F. Bohne, C. *J. Chem., Soc. Chem. Commun.* **1995**, 199−200.

(14) Christoff, M.; Okano, L. R.; Bohne, C. *J. Photochem. Photobiol. A: Chem* **2000**, *134*, 169−176.

(15) Barros, T. C.; Stefaniak, K.; Holzwarth, J. F.; Bohne, C. *J. Phys. Chem. A.* **1998**, *102*, 5639−5651.

(16) Nau, W. M.; Zhang, X. *J. Am. Chem. Soc.* **1999**, *121*, 8022−8032.

(17) Turro, N. J.; Bolt, J. D.; Kuroda, Y.; Tabushi, I. *Photochem. Photobiol.* **1982**, *35*, 69−72.

(18) Hamai, S. *J. Chem. Soc., Chem. Commun.* **1994**, 2243−2244.

(19) Hamai, S. *J. Phys. Chem.* **1995**, *99*, 12109−12114.

(20) Schuh, M. D.; et al. Unpublished results.

(21) Brewster, R. E.; Kidd, M. J.; Schuh, M. D. *J. Chem. Soc., Chem. Commun.* **2001**, 1134−1135.

(22) Park, H.-R.; Mayer, B.; Wolschann, P.; Kohler, G. *J. Phys. Chem. A* **1994**, *98*, 6158−6166.

(23) Almgren, M.; Grieser, F.; Thomas, J. K. *J. Am. Chem. Soc.* **1979**, *101*, 279−291.

(24) Turro, N. J.; Cox, G. S.; Li, X. *Photochem. Photobiol.* **1983**, *37*, 149−153.

(25) Kleinman, M. H.; Bohne, C. In *Organic Photochemistry: Molecular and Supramolecular Photochemistry*; Ramamurthy, V., Schanze, K., Eds.; Marccel Dekker: New York, 1997; Vol. 1, pp 391−466.

(26) Coates, A. I.; Cook, M. P.; Feezor, R.; Schuh, M. D. *J. Inorg. Biochem.* **1998**, *72*, 63−68.

(27) Harata, K. *Bull. Chem. Soc. Jpn.* **1979**, *52*, 1807−1812.

(28) Bertrand, G. L.; Faulkner, J. R., Jr.; Han, S. M.; Armstrong, D. W. *J. Phys. Chem.* **1989**, *93*, 6863−6867.

(29) Rekharsky, M. V.; Inoue, Y. *Chem. Rev.* **1998**, *98*, 1875−1917.

(30) Blyshak, L. A.; Warner, I. M.; Patonay, G. *Anal. Chim. Acta* **1990**, *232*, 239−243.

(31) Castronuovo, G.; Elia, V.; Velleca, F.; Viscardi, G. *Thermochim. Acta* **1997**, *292*, 31−37.

(32) Grabner, G.; Rechthaler, K.; Mayer, B.; Köhler, G.; Rotkiewicz, K. *J. Phys. Chem. A* **2000**, *104*, 1365−1376.

(33) Murphy, R. S.; Bohne, C. *Photochem. Photobiol.* **2000**, *71*, 35−43.